JOURNAL OF GEOPHYSICAL RESEARCH, VOL. 112, D11119, doi:10.1029/2006JD007934, 2007

Local time influence in single-satellite radio occultation climatologies from Sun-synchronous and non-Sun-synchronous satellites

B. Pirscher,[1] U. Foelsche,[1] B. C. Lackner,[1] and G. Kirchengast[1]

Received 18 August 2006; revised 19 February 2007; accepted 1 March 2007; published 13 June 2007.

[1] The sampling error of Global Positioning System (GPS) radio occultation (RO) derived temperature climatologies is computed over a representative time span of 2 years and compared for Sun-synchronous and non-Sun-synchronous Low Earth Orbit (LEO) satellites. The main focus lies on the sampling error's local time component, which is caused by incomplete sampling of the diurnal cycle and which depends on the geometry of the satellite orbits. The Sun-synchronous satellite MetOp (Meteorological Operational European weather satellite) and the non-Sun-synchronous satellite CHAMP (Challenging Minisatellite Payload), both carrying GPS RO instruments on board, serve as representative cases. For the Sun-synchronous satellite MetOp the local time component remains constant during the whole observation period such that the magnitude of the local time errors in monthly mean or longer-term mean RO climatologies is generally lower than ±0.1 K. Except for potential long-term effects of global warming on the diurnal cycle, which might require calibration, this small local time component is stable on decadal timescales and is mainly positive in the Northern Hemisphere and at low latitudes, whereas it is mainly negative in the Southern Hemisphere. These features are attributable to a slight orbit-determined asymmetry in local time sampling. The typical (temporally stable) local time error of an annual mean MetOp climatology resolved into 18 zonal bands amounts to ∼0.04 K. For the non-Sun-synchronous satellite CHAMP the local time error component in monthly mean RO climatologies is also small (up to about ±0.15 K) but more variable (about zero mean) at middle and high latitudes. At low latitudes it results in sinusoidally varying positive and negative deviations with a several-months period, resulting from the local time drift of the satellite. The magnitude of local time errors is slightly larger compared to MetOp since the monthly averaging period is too short for CHAMP to entirely sample a diurnal cycle; a longer averaging period further decreases CHAMP's local time component. An annual mean climatology resolved into 18 zonal bands shows for CHAMP a typical local time residual error component of ∼0.03 K. The overall evidence is that even with single RO satellites, monthly climatologies of high accuracy (sampling error <0.3 K) with the local time component being a minor part (<0.1 K to 0.15 K) can be obtained.

Citation: Pirscher, B., U. Foelsche, B. C. Lackner, and G. Kirchengast (2007), Local time influence in single-satellite radio occultation climatologies from Sun-synchronous and non-Sun-synchronous satellites, *J. Geophys. Res.*, *112*, D11119, doi:10.1029/2006JD007934.

1. Introduction

[2] The Global Positioning System (GPS) radio occultation (RO) method [e.g., *Kursinski et al.*, 1997; *Steiner et al.*, 2001; *Hajj et al.*, 2002] is an active limb sounding technique. Measurements are performed when a GPS receiver mounted in the front or in the aft of a Low Earth Orbit (LEO) satellite tracks a signal of a rising or setting GPS satellite. Because of the satellites' motions, the atmosphere is scanned from bottom up (rising event) or from top to bottom (setting event). Because the GPS signals are modified by the atmosphere depending on its refractive properties, the modifications are a measure for physical atmospheric parameters, in particular refractivity, from which pressure/geopotential height, temperature, and humidity profiles can be derived (see, e.g., *Kursinski et al.* [1997] for details).

[3] The use of radio signals enables measurements to be performed during day and night. The number of measurements depends on the number of transmitters as well as on the number of receivers. Assuming optimal receiver software

[1]Wegener Center for Climate and Global Change and Institute for Geophysics, Astrophysics, and Meteorology, University of Graz, Graz, Austria.

0148-0227/07/2006JD007934$09.00

and antenna characteristics, one single GPS RO receiver can record about 280 RO events per day. Because of insufficient data calibration and data quality not all of them can be translated to useful refractivity, pressure, and temperature profiles [e.g., *Wickert et al.*, 2003, 2006]. Between January 2004 and December 2005 (the period considered within this paper), the WegCenter/University of Graz retrieval of atmospheric profiles from CHAMP (Challenging Minisatellite Payload) RO data yielded on average about 140 high-quality profiles per day.

[4] The potential of RO measurements to provide accurate profiles of atmospheric parameters is already well known in the scientific community. Because of their long-term stability, RO measurements are suitable for climate monitoring and trend detection [*Steiner et al.*, 2001]. The latter use requires all possible error sources, which potentially can induce a trend, to be known with adequate accuracy [*Leroy et al.*, 2006].

[5] A large set of RO measurements enables to create climatologies of atmospheric parameters [e.g., *Borsche et al.*, 2006; U. Foelsche et al., Observing climate with radio occultation data from the CHAMP satellite, submitted to *Climate Dynamics*, 2006, hereinafter referred to as Foelsche et al., submitted manuscript, 2006]. First of all, the validity of these climatologies depends on the reliability of the measurements and its retrieval [e.g., *Hajj et al.*, 2004; *Wickert et al.*, 2004], but it also depends on sampling time and location resulting in the sampling error (Foelsche et al., submitted manuscript, 2006). This paper focuses on the sampling error for single LEO satellites, in particular on the effect of local times at which the RO profiles have been taken.

[6] The local time of RO events depends on the orbit of the receiver satellite. A GPS receiver mounted on a LEO satellite with high inclination allows for measurements to be performed at every position on the globe. During one revolution, the LEO subsatellite track crosses each geographical latitude at two different local times. At the equator, the local times are separated by twelve hours, but the higher the latitude the more asymmetric are the subsatellite points in local time.

[7] Sun-synchronous satellites are a particular type of LEO satellites. They are characterized by unchanging equator crossing times [*Larson and Wertz*, 1997]. The equator crossing times of non-Sun-synchronous satellites change depending on their rate of nodal precession (section 2 provides more details). For this reason only non-Sun-synchronous satellites are able to entirely sample a diurnal cycle of a measurand. Satellites with very slow drifting rates (some hours within some years) are most unfavorable in regard to local time sampling and climate trend detection. As experience with Microwave Sounding Unit (MSU) climate time series has shown, such a long-term drift can pretend a false trend in the time series [*Mears and Wentz*, 2005].

[8] The satellite orbit-dependent influence on local time sampling has already been investigated in relation to global cloud imagery data [*Salby and Callaghan*, 1997] and to brightness temperatures [*Kirk-Davidoff et al.*, 2005]; an extensive theoretical study was also performed by *Leroy* [2001]. Here, we focus on temperature data as obtainable from radio occultation, i.e., gathered at times and locations of GPS RO events.

[9] A description of properties of Sun- and non-Sun-synchronous satellite orbits and their implications on radio occultation measurement times and locations are given in section 2. In addition, the mathematics of the sampling error estimation as well as the separation of its local time component are introduced. The characterization of sampling error and local time component properties in RO temperature climatologies is presented in section 3 and section 4 closes with summary and conclusions.

2. Methods

[10] The total error of RO climatologies can be separated into an observational and a sampling error component [*Foelsche et al.*, 2006, also submitted manuscript, 2006]. The latter can be estimated, when the times and locations of RO events are known. The use of an adequate reference atmosphere enables the sampling error to be estimated even for future missions knowing their orbit characteristics.

[11] We investigated the sampling error (SE) of RO climatologies and its local time component (LTC) for the non-Sun-synchronous satellite CHAMP [*Wickert et al.*, 2001] and the Sun-synchronous satellite MetOp [*Loiselet et al.*, 2000]. CHAMP has been in orbit since 15 July 2000, and has been continuously recording RO data since September 2001. MetOp-A (the first of three MetOp satellites) was launched on 19 October 2006, the full MetOp series bound to operationally deliver GPS RO data until 2020.

[12] To be independent from RO observational errors, we exclusively used colocated ECMWF (European Centre for Medium-Range Weather Forecasts) profiles to estimate the sampling error (see section 2.2). For obtaining the event distribution of real CHAMP profiles, colocated ECMWF profiles were extracted at times and locations of RO events for all events where the real RO data passed the quality control within the Wegener Center CHAMP retrieval (real-CHAMP). Moreover, ECMWF profiles were extracted where simulations of CHAMP and MetOp yielded RO events (simCHAMP and simMetOp, respectively). The simulations of simCHAMP and simMetOp radio occultation events (times and locations) were performed using the End-to-end Generic Occultation Performance Simulator (EGOPS) [*Kirchengast et al.*, 2004] with appropriate satellite orbit element files for CHAMP and the MetOp orbit. For these simulated RO profiles no special "quality control loss" of a fraction of the profiles was found worthwhile to consider so that all theoretically feasible RO events were used in further examinations.

[13] The investigations were performed on the basis of a period of 2 years from January 2004 until December 2005, a time span sufficiently long to also test for any potential longer-term secular components in the sampling characteristics.

2.1. Satellite Orbits

[14] The CHAMP satellite flies in a non-Sun-synchronous orbit with an inclination of 87.2° and an initial altitude of 454 km (July 2000) [*Wickert et al.*, 2001]. From January 2004 until December 2005 its altitude decreased from about 385 km to 345 km. The Sun-synchronous satellite MetOp is situated in an orbit with 98.7° inclination and an altitude of

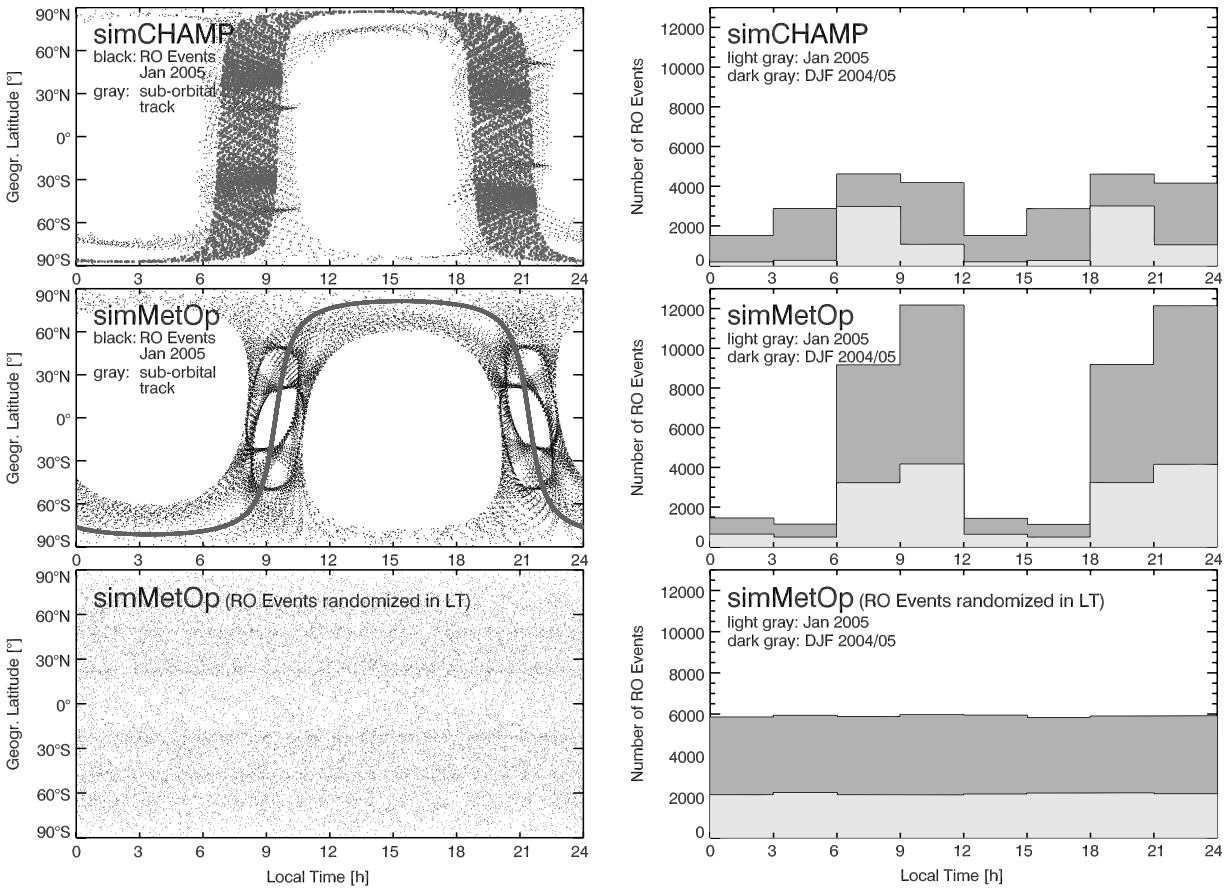

Figure 1. (left) Occultation locations (black dots) and satellite suborbital tracks (gray) in January 2005. (right) Number of measurements as function of local time in January 2005 (light gray) and DJF 2004/2005 (dark gray) of simCHAMP, simMetOp and randomized simMetOp.

about 830 km, with MetOp's equator crossing (descending node) at 0930 local time; the orbit will be maintained at the nominal local time within the satellite life time.

[15] The Earth's oblateness is the main reason for secular drift in satellite orbit planes. Assuming a circular orbit, an orbit's precession rate $\dot{\Omega}$ [rad s^{-1}] can be calculated as

$$\dot{\Omega} = -\frac{3}{2} J_2 \left(\frac{a_e}{a}\right)^2 n \cos i, \tag{1}$$

where $J_2 = 1082.63 \times 10^{-6}$ is the negative of the second zonal coefficient of spherical harmonics describing the Earth's polar oblateness, $a_e = 6378.137$ km is the mean equator radius of the Earth, a is the semimajor axis of the satellite's orbit, i its inclination, and $n = \sqrt{GM_e/a^3}$ is the mean motion of the satellite [rad s^{-1}], where $G = 6.67 \times 10^{-11}$ m^3 kg^{-1} s^{-2} is the gravitational constant and $M_e = 5.97 \times 10^{24}$ kg the mass of the Earth [*Hoffmann-Wellenhof et al.*, 1997; *Larson and Wertz*, 1997; *Boain*, 2005].

[16] The orbit parameters i and a can be chosen in a way that the precession rate of the satellite equals to the mean motion of the Earth on the way around the Sun. The mean motion of the Earth amounts to 360°/365.242199 d = 0.9856°/d. If $\dot{\Omega}$ = 0.9856°/d, the satellite circuits on a Sun-synchronous orbit. A Sun-synchronous orbit can be obtained by different possible combinations of a and i, whereby a higher orbital altitude requires a slightly lower inclination (see equation (1)). If $\dot{\Omega}$ is greater or less than 0.9856°/d, the satellite drifts in local time.

[17] Applying equation (1) to the orbit parameters of CHAMP, the local time drifting rate increases from one hour in 10.9 days in January 2004 to one hour in 10.8 days in December 2005. The reason for this change is the decrease in its altitude due to atmospheric drag. Overall, the local time drift of CHAMP's orbit amounts to about three hours per month. Figure 1 (top left) illustrates the subsatellite points (gray dots) of CHAMP in January 2005 (plotted at each time when a RO event occurred). Within this month, the local time of the descending node shifted from 0940 to 0645 local time. Since RO measurements can be performed during day and night, the full diurnal cycle is sampled within about 130 days. That implies that neither a monthly nor a seasonal period suffices to entirely sample over all local times (Figure 1, top).

[18] Since satellites in Sun-synchronous orbits are characterized by fixed equator crossing times they are not able to fully resolve the diurnal cycle at low and midlatitudes (Figure 1, middle). The local time of MetOp's descending node (equator crossing time) remains constant at 0930 local time (in practice foreseen to be maintained to ±5 min accuracy).

[19] The stability of the Sun-synchronous orbit and its asymmetry regarding local time sampling at high latitudes

leads to an unequal weighting of day and night in the Northern and Southern Hemisphere (Figure 1, middle left), which will be important to interpret potential local time errors (section 3). Even though the limb sounding of RO measurements somewhat spreads the local time at which measurements are performed (Figure 1, middle) the majority of the measurements at middle and high northern latitudes is performed during daytime, whereas at middle and high southern latitudes most of them take place during nighttime. At 60°N, for example, the local times of the MetOp subsatellite points are at about 1030 and 2020 local time, respectively, but the measurements take place from 0730 until 2230 local time.

[20] Figure 1 (right) depicts the number of simCHAMP and simMetOp measurements as a function of local time. The considerable difference of total event numbers results from CHAMP only observing setting occultations (only one aft-looking antenna) whereas MetOp observes about twice as many occultations, using setting and rising events (one front- and one aft-looking antenna). The local time drift of CHAMP causes a more even distribution of RO events in local time when extending the time span from month to season (Figure 1, top left). MetOp stays stationary in local time sampling so that independent of the considered time interval (month or season), the event's local time will be the same: only the number of measurements will change (Figure 1, middle right).

[21] The event distribution of realCHAMP is similar to the one of simCHAMP but the number of realCHAMP events is evidently reduced because of the restriction to events where real CHAMP profiles of high quality exist.

2.2. Sampling Error Calculation

[22] Global large horizontal-scale RO climatologies of atmospheric parameters, if they shall be independent of models or other external data, are created from a set of RO measurements gathered into "bins" (geographical cells). A "bin" corresponds to the spatial resolution of the climatology. In the WegCenter standard setup for single-satellite climatologies [*Borsche et al.*, 2006] the spatial resolution refers to zonal bands with 10° latitudinal extension. The vertical sampling we use is 500 m (original data set 200 m) up to 35 km, the temporal resolution corresponds to one month.

[23] RO climatologies exhibit some differences relative to other selected reference data sets, e.g., to ECMWF or NCEP (National Centers for Environmental Prediction) [*Gobiet et al.*, 2005; *Lackner and Pirscher*, 2005]. Important in this study are those caused by irregularly distributed RO sampling times and locations. That is even perfect measurements (no observational error) yield a SE in the climatology; the use of perfect measurements (in simulation) permits an estimate of the SE.

[24] In our investigation ECMWF fields are used to extract proxy profiles for perfect RO measurements as well as to provide a quasi realistic reference atmosphere. ECMWF fields have a temporal resolution of 6 hours and are used at a spatial resolution of T42 (horizontal resolution of ~300 km). The horizontal resolution is selected to match the natural horizontal averaging of RO profiles, which is ~300 km as well [*Kursinski et al.*, 1997].

[25] In a first step the time of the RO event is allocated to the nearest ECMWF time layer. ECMWF fields are available at four time layers (0000 UTC, 0600 UTC, 1200 UTC, and 1800 UTC) so that RO events are always shifted in time by less than three hours. This temporal adjustment in UTC also yields corresponding shifts in local time, so that the use of ECMWF data at its four time layers does not perfectly reproduce the real RO SE and the real LTC (still we find it the best available data set for the purpose). In the case of simMetOp, for example, the temporal allocation of ECMWF profiles results in the RO profiles to be more widely distributed with respect to local time compared to Figure 1 (middle right). Thus the LTC estimation will generally miss some variability compared to real RO measurements. Furthermore we are aware that the four ECMWF time layers do not represent an optimal sampling of all harmonics of the diurnal cycle. However, four time layers are sufficient to sample the diurnal cycle up to the second harmonics (the semidiurnal variations) so that the major components are captured by the LTC estimation and the residual delta error missed in our LTC estimates will be of first order (10% level) only.

[26] After shifting the RO event to the nearest neighbor time layer, the ECMWF field is spatially interpolated to the geographic RO event location, where the proxy RO profile is extracted.

[27] Mathematically, the SE is computed in forming the difference between an average of all colocated RO profiles within one bin, $\overline{T(z,\varphi)^{\mathrm{prof}}}$, and the "true" mean of the bin, $\overline{T(z,\varphi)^{\mathrm{true}}}$,

$$\Delta T(z,\varphi)^{\mathrm{SE}} = \overline{T(z,\varphi)^{\mathrm{prof}}} - \overline{T(z,\varphi)^{\mathrm{true}}}, \tag{2}$$

where T is the atmospheric parameter (temperature), z is the height, and φ denotes the mean geographic latitude of the bin.

[28] Practically, $\overline{T(z,\varphi)^{\mathrm{prof}}}$ is first calculated for 5° zonal bands being the chosen fundamental bin size, from averaging all individual colocated RO profiles within the zonal band, weighted with the cosine of their latitudes. The "true" mean profile $\overline{T(z,\varphi)^{\mathrm{true}}}$ is obtained by averaging temperature profiles at all grid points in the fundamental bin (again weighted with the cosine of the latitude) and all time layers within the selected time interval.

[29] When averaging the horizontal resolution from the fundamental 5° zonal bins to larger destination bins (first of all to our basic resolution of 10° zonal bands but also up to a global overarching bin as used in section 3.3), each mean colocated profile and each "true" mean profile is weighted with its corresponding fundamental bin area. Afterward, the sampling error is calculated for all destination bins as difference between the mean colocated profile and the mean reference profile (equation (2)).

[30] If instead of zonal averaging longitudinal sectors are considered (as in one comparison case in section 3.2.2 and section 3.3) it is straightforward to apply equation (2) to any given longitudinal dimension of the bin only.

[31] The SE contains a random and a systematic component. The random component of the SE is caused by atmospheric variability, which is not adequately sampled by the satellite. An absence of data due to a temporal lack of measurements, for example, results in an inhomogeneity in temporal sampling. The absence of data of one week in

January, for example, could cause a significantly increased SE in a January climatology. However, the random component of the sampling error is increasingly reduced by averaging over longer timescales and/or larger spatial regions as well as by increasing spatial and temporal density of observations if so becoming available.

[32] The systematic component of the SE results from systematic spatial and temporal undersampling. The spatial component stems from an inhomogeneous spatial sampling. To give an example, few measurements are taken between 85°N/S and 90°N/S. The reason for this is the small inclination of GPS satellites ($i \approx 55°$), which renders measurements beyond 85° latitude very sparse.

[33] MetOp's systematic undersampling of the diurnal cycle (the SE's LTC) can be attributed to the satellite's orbit. A Sun-synchronous satellite always samples at the same local times, whereas a non-Sun-synchronous satellite samples at all local times if the averaging period is long enough. The systematic component of the sampling error cannot be entirely removed by increasing the number of measurements because the satellites sampling pattern remains the same over time. Since the diurnal cycle also contains day-to-day variability, the LTC does have a random component which reduces when a larger number of measurements is used.

[34] In order to estimate the LTC (i.e., essentially the influence of the diurnal and semidiurnal cycles) as part of the SE, the SE of the colocated ECMWF temperature profiles is taken as basis from which the nonlocal time SE calculated from ECMWF profiles taken at the same location at the same (UTC) day, but at randomized times of the day is subtracted (Figure 1, bottom):

$$\Delta T(z,\varphi)^{\mathrm{LTC}} = \Delta T(z,\varphi)^{\mathrm{SE}} - \Delta T(z,\varphi)^{\mathrm{SE\ rand}}. \tag{3}$$

[35] It is evident from Figure 1 (bottom right) that the artificially randomized distribution is flat over all local times, i.e., well mimics a baseline sampling without local time selectiveness.

[36] In order to estimate the typical magnitude of the SE and its LTC for RO climatologies gridded at some given space-time resolution within larger geographical regions, resolution-specific mean SE and mean LTC magnitudes are computed for such larger regions. The baseline resolution we focus on is monthly zonal mean climatologies resolved into 18 zonal bands (10° latitudinal width) and 500 m height gridding. Regarding the height gridding, the SE and LTC estimates will also be valid for any gridding finer than 500 m, since the underlying RO profiling data have ~1 km vertical resolution (further smoothed by the averaging into bins), so that <500 m oversampling will not add to mean SE/LTC magnitudes.

[37] Climatologies with other complementary resolutions of interest are assessed as well (see section 3 below), such as with seasonal instead of monthly averaging, at the same spatial resolution. CHAMP RO climatologies of the baseline resolution, and alternatively with seasonal averaging, have been exploited, for example, in studies by *Gobiet et al.* [2005], *Foelsche et al.* [2006, also submitted manuscript, 2006], and *Borsche et al.* [2007]. The realCHAMP SE/LTC estimates in the present study are thus directly applicable to these climatologies (which will be publicly available via Web site as of summer 2007).

[38] For any climatology at a given spatial resolution, we estimate the resolution-specific mean SE and mean LTC magnitudes for larger regions, $\Delta T(z,\varphi)^{\mathrm{ResolMean\ SE}}$ and $\Delta T(z,\varphi)^{\mathrm{ResolMean\ LTC}}$, via averaging the magnitudes (absolute values) of $\Delta T(z,\varphi)^{\mathrm{SE}}$ and $\Delta T(z,\varphi)^{\mathrm{LTC}}$ from all relevant climatology grid points,

$$\Delta T(z,\varphi)^{\mathrm{ResolMean\ SE}} = \frac{1}{N_{\mathrm{grid}}} \sum_{i=1}^{N_{\mathrm{grid}}} \left| \Delta T(z,\varphi)^{\mathrm{SE}} \right|, \tag{4}$$

$$\Delta T(z,\varphi)^{\mathrm{ResolMean\ LTC}} = \frac{1}{N_{\mathrm{grid}}} \sum_{i=1}^{N_{\mathrm{grid}}} \left| \Delta T(z,\varphi)^{\mathrm{LTC}} \right|, \tag{5}$$

where N_{grid} specifies the number of grid points within a defined larger region (definitions in section 3). The SHP/LS (Southern Hemisphere polar, lower stratosphere) region, for example, ranges from 60°S to 90°S. With 10° latitudinal sampling (bin size), and from an altitude of 15.5 km to 35.0 km with 500 m vertical sampling, this yields a total number of grid points $N_{\mathrm{grid}} = 120$.

[39] Complementary information on the residual error in larger domains is obtained from the calculation of direct region-average values. These region-averages, $\Delta T(z,\varphi)^{\mathrm{RegionMean\ SE}}$ and $\Delta T(z,\varphi)^{\mathrm{RegionMean\ LTC}}$ obtained from expressions equivalent to equations (4) and (5) but without taking absolute values of $\Delta T(z,\varphi)^{\mathrm{SE}}$ and $\Delta T(z,\varphi)^{\mathrm{LTC}}$, enable to quantify how the average errors approach zero, or a residual systematic bias, when averaging over increasingly larger space-time domains.

[40] In summary, both types of mean SE/LTC estimates have their value, the resolution-specific one to characterize over larger regions the typical SE/LTC of climatologies at prespecified spatial grids (the primary focus of this paper), the region-average one to assess what the residual SE/LTC errors are for increasingly larger space-time averaging.

3. Results and Discussion

3.1. Features of Sampling Error and Local Time Component

[41] Figure 2 depicts the temperature SE (left) and its LTC (right) in January 2005 to illustrate the SE and LTC of a single month at the basic climatological resolution (10° zonal bands). The SE characteristics of realCHAMP, simCHAMP, and simMetOp are quite similar. The latitudinal behavior of the SE is associated with the extent of underlying temperature variability. At low latitudes temperature variations are less pronounced but the higher the latitudes, the larger are the temperature variations and thus the larger are generally the effects on the SE [*Foelsche et al.*, 2006, also submitted manuscript, 2006]. The salient positive SE at middle and high northern latitudes in January 2005 (which is the worst case in the Northern Hemisphere within the 2 years considered) is attributable to the undersampling of the polar vortex, where spatiotemporal variability is particularly strong.

[42] The measurements' local time is associated with the satellite's equator crossing time. The equator crossing time

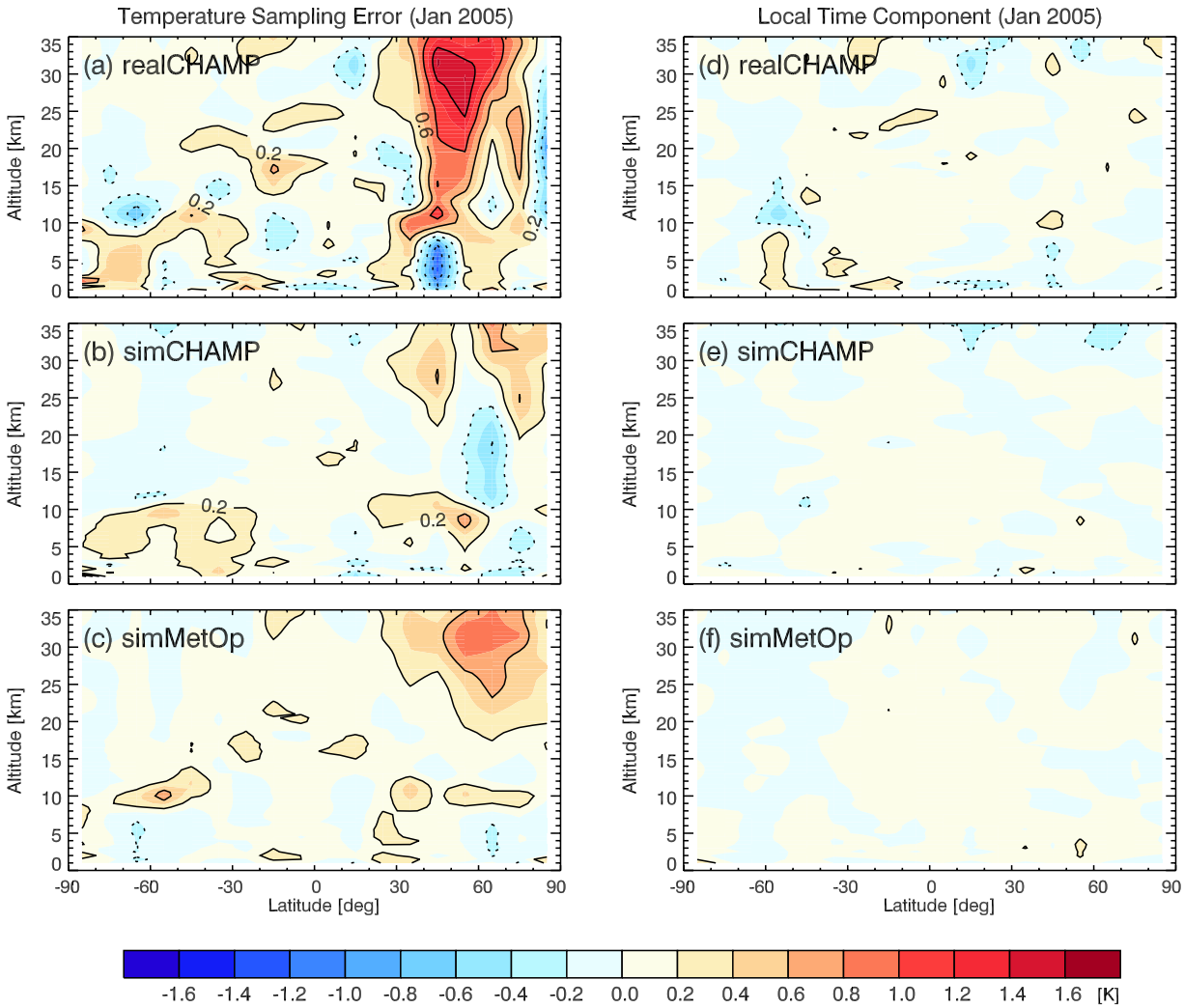

Figure 2. (left) Monthly zonal mean temperature sampling error and (right) respective local time component of the error in January 2005.

of the Sun-synchronous satellite MetOp always keeps constant at 0930 local time (descending node). CHAMP's equator crossing time shifted from approximately 0940 to 0645 local time in January 2005. The close similarity of MetOp's and CHAMP's LTC (Figure 2, right) can be attributed to the similar equator crossing times during this particular month. The absolute magnitude of the LTC is, in general, less than 0.1 K. realCHAMP's maximum values are larger and regions with a more pronounced LTC are somewhat wider spread than in case of simCHAMP. This is due to the reduced number of real measurements, since an increase in the number of profiles reduces the random component of the sampling error's LTC.

[43] In order to show the systematic behavior of the SE and its LTC in the tropics (20°S to 20°N, TRO) and in the Southern Hemisphere subtropics and midlatitudes (20°S to 60°S, SHSM), respectively, Figure 3 depicts the temporal evolution of region-average SE and region-average LTC for the full 2 years simulated (realCHAMP top, simMetop bottom). CHAMP's tropical SE resembles a pattern with sinusoidally varying positive and negative deviations, most pronounced between an altitude of 5 km and about 25 km. Above a height of about 27 km it is predominantly negative. The tropical SE of simMetOp stays mainly positive with some increase of the SE between an altitude of 16 km and 20 km around the tropopause (at some spots exceeding 0.2 K).

[44] This increase in tropopause region variability is very clearly visible in the SE in the SHSM region for both realCHAMP and simMetOp, at altitudes from about 8 km to 13 km. This region shows a SE > 0.2 K observable during almost the whole observation period. This results from the comparatively larger temperature variability around the tropopause [*Borsche et al.*, 2007].

[45] The feature is readily identifiable as well in real-CHAMP's tropical SE (Figure 3, top left) but there the overlay of the LTC is sufficiently strong that the positive deviation is cyclically broken when the measurement's local time results in a negative LTC.

[46] In general, the local time-dependent part of the SE is well discernible in the respective SE error in the tropics. In case of realCHAMP, whose measurements drift in local time, the tropical LTC shows a cyclic positive and negative deviation within ±0.1 K, a full cycle spanning about four

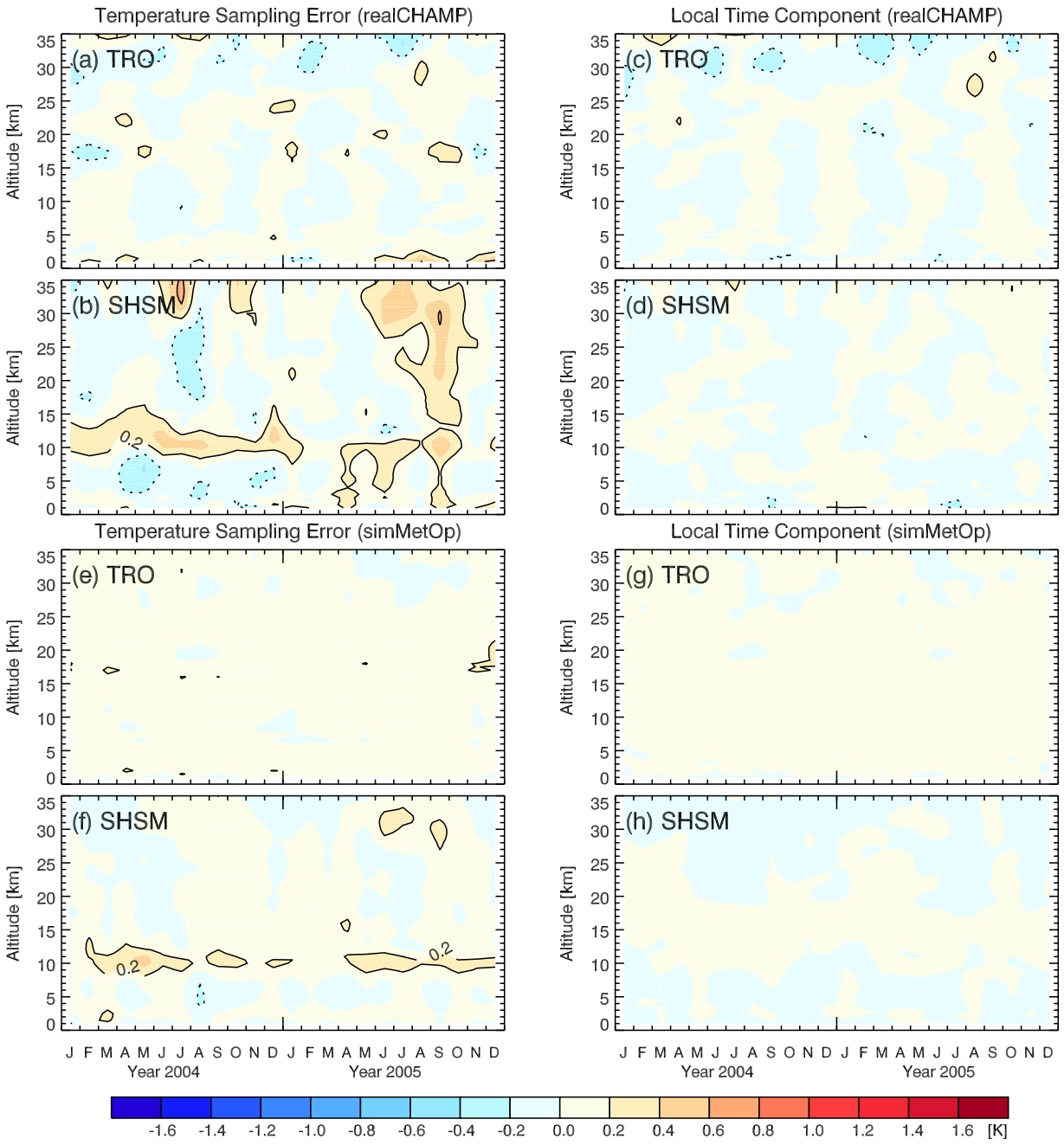

Figure 3. Time series of (left) the monthly region-average temperature sampling error and (right) the local time component of the error of (a–d) realCHAMP and (e–h) simMetop. TRO corresponds to the tropical band from 20°S to 20°N, and the Southern Hemisphere subtropics and midlatitudes (SHSM) represent the region from 20°S to 60°S.

months. This pattern is synchronous with the local time drift of CHAMP RO profiles, aligned with the drifting CHAMP orbit and determined by the 130 days period per one full diurnal cycle (see section 2.1).

[47] At low latitudes the Sun-synchronous satellite MetOp almost everywhere keeps a small positive LTC (smaller than +0.1 K) during the whole observation period. This results from the equator crossing times of MetOp, which are at 0930/2130 local time (descending and ascending node). For this reason most events take place between 0800/2000 and 1100/2300 local time and no events occur between 0000/1200 and 0700/1900 local time. Thus the skew-symmetric diurnal temperature cycle causes the LTC to be slightly positive compared to full local time sampling. This systematic bias can be expected to be persistent over the lifetime of MetOp.

[48] As mentioned above the larger temperature variability at middle and high latitudes causes the SE to be more pronounced there compared to low latitudes (see Figure 2, high northern latitudes). This SE, which occurs in hemispheric winter months, is also recognizable in Figures 3b

and 3f in the SHSM region. The largest SE occurs in the winter polar region, but it rarely exceeds ±1.0 K.

[49] The LTC part of the SE diminishes at higher latitudes. Partly this results from the strong temperature variability, which exceeds the LTC, and partly it results from a decrease of the LTC with latitude. The geometry of the orbits allowing for measurements to be performed within a larger range of local times (see Figure 1) at high latitudes may contribute to this decrease of LTC as well as the fact that amplitudes of thermal tides of the atmosphere cause the diurnal cycle to be strongest in the tropics.

[50] CHAMP's general LTC behavior outside the tropics in both hemispheres is characterized by quasi-random positive and negative deviations (smaller than ±0.1 K) during the observation period (see Figure 3d).

[51] MetOp's LTC is different in the extratropical Northern and the Southern Hemisphere. The Northern Hemispheric LTC is affected by more RO events during daytime (see Figure 1, middle left), which results in a positive LTC (generally smaller than +0.1 K though), whilst the counterpart behavior is formed in the Southern Hemisphere (Figure 3h), where the oversampling during nighttime yields a systematic negative contribution outside of ∼10 km to ∼20 km (smaller than −0.1 K though). This shows that the first harmonic of the diurnal cycle (period of 24 hours) cannot be removed completely at high latitudes because of the systematic asymmetry in observational time following from the satellite's Sun-synchronous orbit [*Leroy*, 2001]. Because of the stability of the orbit, the LTC keeps highly correlated overall within the latitudinal region also in the long term [*Kirk-Davidoff et al.*, 2005].

3.2. Absolute Amount of Sampling Error and Local Time Component

3.2.1. Typical Values for Some Subdomains

[52] Figure 4 depicts the temporal variations of the resolution-specific SE and the resolution-specific LTC of the error (equations (4) and (5)) for realCHAMP (gray) and simMetOp (black), respectively, for a range of subdomains of the global atmosphere. Table 1 supplements these graphical results with numerical values, showing the 2 year average in all different latitudinal regions and different height ranges considered. These values represent typical values, which have to be expected within the subdomains when looking at a monthly climatology resolved into 18 zonal bands (10° latitudinal width) and 500 m (or smaller) height gridding.

[53] The domains NHP/SHP (Northern/Southern Hemisphere polar) represent 60°N/S to 90°N/S, NHSM/SHSM (Northern/Southern Hemisphere subtropics and midlatitudes) denote 20°N/S to 60°N/S, and TRO means the tropical region between 20°N and 20°S. The height ranges are divided into LS (lower stratosphere, height range between 15 km and 35 km), UT (upper troposphere, 5 km to 15 km), and LT (lower troposphere, 1 km to 5 km), respectively.

[54] The comparison between realCHAMP and simCHAMP values allows for conclusions concerning the influence of the number of measurements, which are incorporated in the SE calculations. The same in principle applies for a comparison between simCHAMP and simMetOp data but these satellites also differ in their orbital characteristics.

[55] Figure 4 and Table 1 show that the resolution-specific SE's and LTC's temporal development as well as their magnitudes are in general similar for all satellites. Nevertheless, it is evident that a larger number of observations decreases both the SE and its LTC. A significant difference between Sun- and non-Sun-synchronous orbits cannot be observed; it has to be kept in mind that CHAMP is far from covering one full diurnal cycle within one month. Thus the additional decrease in SE and LTC from simCHAMP to simMetOp is mostly attributable to the increase in the number of measurements.

[56] Figure 4 and Table 1 also show that the SE has a relatively symmetric appearance with respect to the equator. Seasonal temperature variations amplify the error in hemispheric winter, whereas it is lowest in the tropical region. In general, no remarkable height-dependent pattern is noticeable. Sole exception is the SHP/LT region where large SE values can be found. The reason for this special SE is the presence and topography of the Antarctic continent, which allows only few RO profiles to extend to sea level and cuts many near 4 km height above the Antarctic plateau. The few low-reaching profiles are systematically warmer than the full average, resulting in that comparatively larger deviation.

[57] The temporal behavior of the LTC error part of the SE (Figure 4, right) is different from the SE. Even though a seasonal cycle is observable at high latitudes (larger LTC in hemispheric winter), comparatively large LTC magnitudes also occur at tropical latitudes, where the diurnal cycle is most pronounced. A special feature occurs in the tropical lower stratosphere (TRO/LS), where the estimated LTC is about the same size as the respective SE (see Table 1). The reason for this is a small residual estimation error, which the application of equations (3) to (5) can leave in case of small SE error magnitudes and if the SE is dominated by the LTC: The standard deviation of the difference of the partly uncorrelated grid values (one from the standard, one from the randomized simulation) can be larger (theoretically up to a factor of $\sqrt{2}$) than the standard deviation of the original grid values. If the SE, for example, shows a positive sign and the randomized SE shows a negative sign, the absolute value of the difference between both factors is larger than the absolute value of the factors themselves.

3.2.2. Typical Values for the Global UTLS

[58] The study of SE properties was proceeded by investigating the error in the UTLS region (upper troposphere lower stratosphere, altitude range between 5 km and 35 km): Resolution-specific SE and LTC were calculated in a monthly 60° longitudinal UTLS sector (between 15°W and 45°E, i.e., in total one sixth of the global area), and in the monthly and seasonally global UTLS region. The latitudinal resolution corresponds to our standard resolution of 10°, the vertical resolution still is 500 m (5 km to 35 km) in any case. Seasonal climatologies cover the period from DJF 2003/2004 until SON 2005. Figure 5 depicts the results and Table 2 summarizes the 2-year average values. In Table 2 also the values for the average annual mean have been added.

[59] Overall the climatologies are of high accuracy with average SE smaller than 0.3 K and average LTC smaller than 0.15 K, respectively. The comparison between the monthly 60° sector mean and the monthly zonal mean allows to see the spatial resolution dependency of the mean SE. Insight into its temporal resolution dependency can be gained by comparing

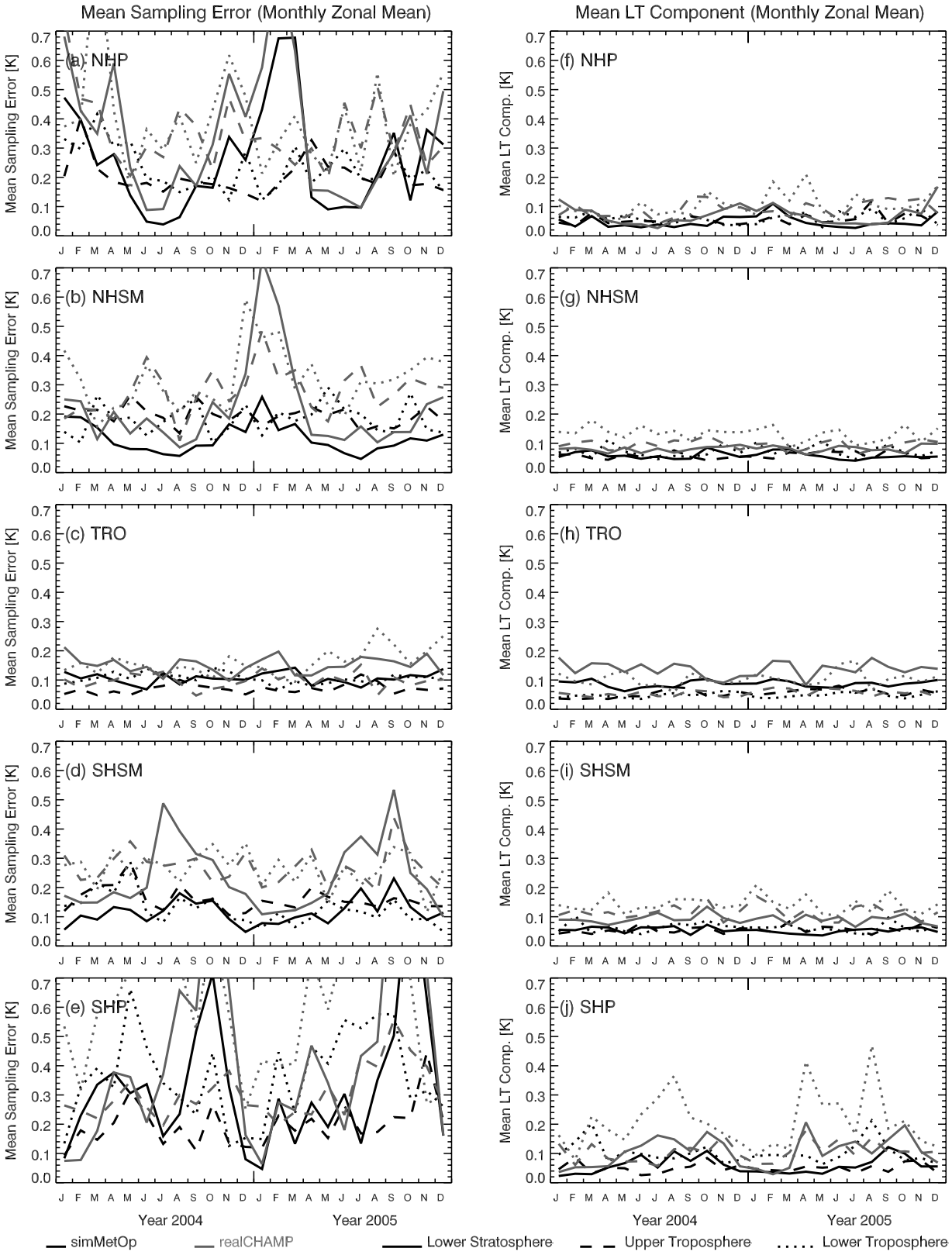

Figure 4. Time series of (left) the resolution-specific mean sampling error and (right) the resolution-specific mean local time component of the error in five different latitudinal regions (rows) for three different height regions (line styles) of realCHAMP (gray) and simMetOp (black). For detailed definition of regions, see text.

Table 1. Two-Years Average of Resolution-Specific Sampling Error [K] and Resolution-Specific Local Time Component of the Error [K] in Five Different Latitude Regions for Three Different Height Regions of realCHAMP, simCHAMP, and simMetOp[a]

	SHP		SHSM		TRO		NHSM		NHP	
	SE	LTC	SE	LTC	SE	LTC	SE	LTC	SE	LTC
realCHAMP										
$LS_{ResolMean}$	0.44	0.11	0.24	0.09	0.15	0.14	0.22	0.08	0.35	0.07
$UT_{ResolMean}$	0.31	0.11	0.27	0.12	0.10	0.05	0.28	0.10	0.35	0.09
$LT_{ResolMean}$	0.61	0.21	0.26	0.14	0.16	0.10	0.32	0.13	0.40	0.11
simCHAMP										
$LS_{ResolMean}$	0.31	0.07	0.16	0.06	0.12	0.11	0.14	0.06	0.21	0.05
$UT_{ResolMean}$	0.19	0.06	0.19	0.07	0.08	0.05	0.21	0.06	0.22	0.07
$LT_{ResolMean}$	0.40	0.14	0.17	0.09	0.14	0.09	0.23	0.10	0.24	0.07
simMetOp										
$LS_{ResolMean}$	0.33	0.06	0.12	0.05	0.11	0.09	0.12	0.06	0.26	0.05
$UT_{ResolMean}$	0.20	0.05	0.16	0.06	0.07	0.05	0.20	0.06	0.20	0.06
$LT_{ResolMean}$	0.36	0.10	0.13	0.06	0.11	0.05	0.18	0.07	0.23	0.06

[a]For detailed definition of regions, see text.

Table 2. Two-Years Average of Resolution-Specific Sampling Error [K] and Resolution-Specific Local Time Component of the Error [K] Calculated in the UTLS Region With Different Spatial and Temporal Resolutions of the Climatological Data

	real-CHAMP		sim-CHAMP		simMetOp	
	SE	LTC	SE	LTC	SE	LTC
Monthly 60° sector ResolMean	0.38	0.17	0.27	0.12	0.24	0.09
Monthly zonal ResolMean	0.25	0.10	0.17	0.07	0.17	0.06
Seasonal zonal ResolMean	0.18	0.06	0.12	0.04	0.12	0.05
Annual zonal ResolMean	0.11	0.03	0.07	0.02	0.08	0.04

monthly, seasonal, and annual zonal means. The influence of the number of profiles on the errors can be best seen at any given resolution, from the difference between realCHAMP and simCHAMP. The satellite's orbit characteristics are reflected in different decreases in the resolution-specific SE and its LTC for CHAMP and MetOp, respectively.

[60] The resolution-specific SE decreases by about two thirds from the coarsest to the most detailed resolved data set. The spatial enlargement from the 60° sector mean to the

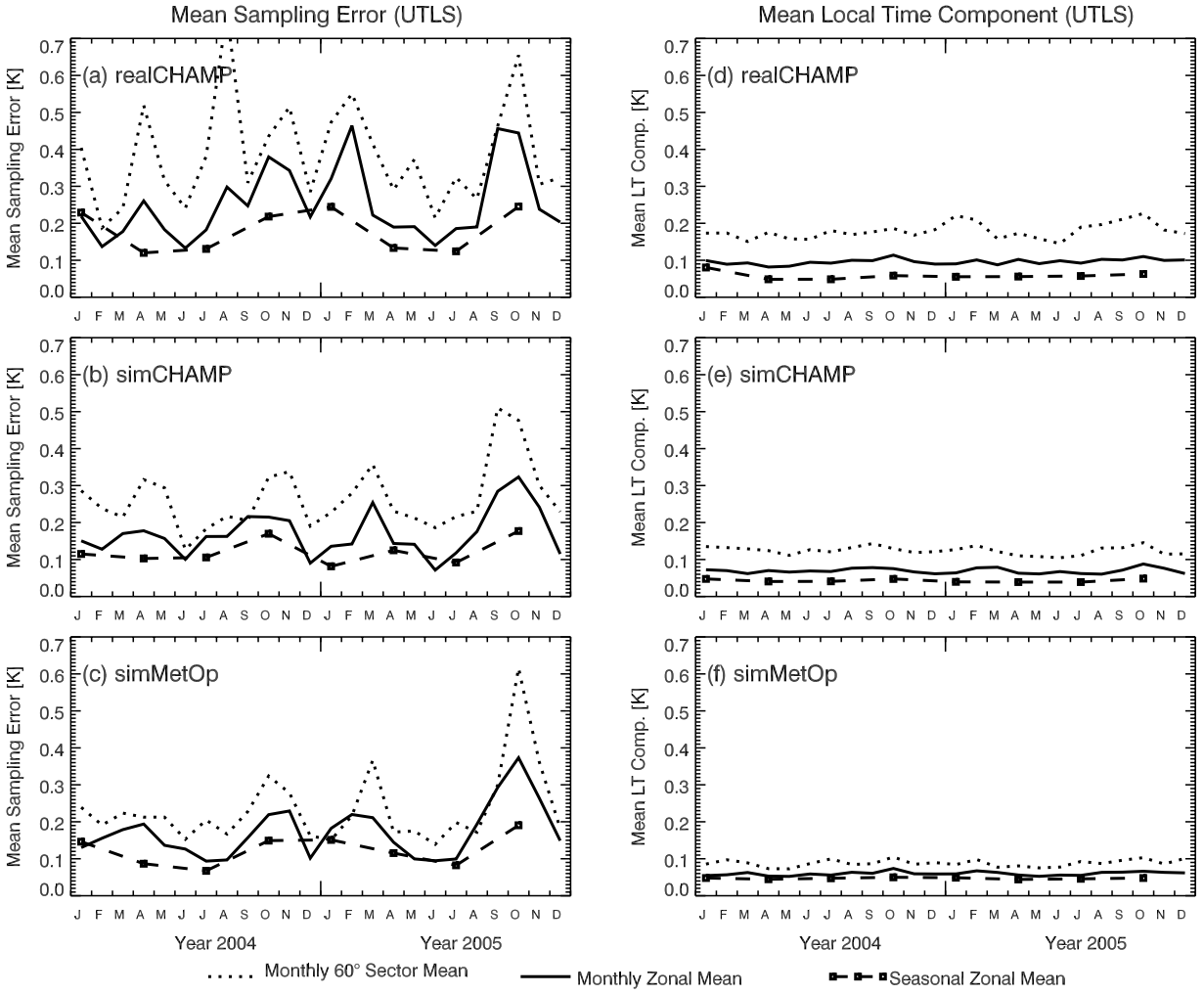

Figure 5. Time series of (left) the UTLS region resolution-specific mean sampling error and (right) the resolution-specific mean local time component of the error for monthly averages in a 60° longitudinal sector (dotted), monthly zonal averages (solid), and seasonal zonal averages (dashed), respectively.

Table 3. Two-Years Average and Standard Deviation of Region-Average Sampling Error [K] and Region-Average Local Time Component of the Error [K] in Five Different Latitude Regions for Three Different Height Regions of realCHAMP, simCHAMP, and simMetOp

	SHP		SHSM		TRO		NHSM		NHP	
	SE	LTC	SE	LTC	SE	LTC	SE	LTC	SE	LTC
					realCHAMP					
$LS_{RegionMean}$	0.06	0.00	0.05	0.00	0.00	−0.02	0.07	0.00	0.16	0.00
$UT_{RegionMean}$	0.01	0.01	0.03	0.00	0.00	0.00	0.03	0.00	0.03	0.00
$LT_{RegionMean}$	0.02	0.00	0.00	0.00	0.01	0.00	0.01	0.00	0.00	0.00
$LS_{RegionStdDev}$	0.35	0.06	0.13	0.05	0.06	0.06	0.14	0.03	0.27	0.03
$UT_{RegionStdDev}$	0.07	0.02	0.03	0.01	0.02	0.01	0.03	0.01	0.06	0.01
$LT_{RegionStdDev}$	0.03	0.02	0.02	0.01	0.01	0.01	0.02	0.01	0.05	0.01
					simCHAMP					
$LS_{RegionMean}$	0.13	0.00	0.05	0.00	0.01	−0.01	0.02	0.00	0.08	0.00
$UT_{RegionMean}$	0.00	0.00	0.03	0.00	0.00	0.00	0.03	0.00	0.02	0.00
$LT_{RegionMean}$	−0.01	0.00	0.00	0.00	0.01	0.00	0.02	0.00	−0.01	0.00
$LS_{RegionStdDev}$	0.25	0.02	0.06	0.03	0.06	0.07	0.07	0.03	0.14	0.03
$UT_{RegionStdDev}$	0.03	0.01	0.01	0.01	0.02	0.01	0.02	0.01	0.03	0.01
$LT_{RegionStdDev}$	0.01	0.01	0.01	0.01	0.01	0.00	0.01	0.00	0.03	0.01
					simMetOp					
$LS_{RegionMean}$	0.10	−0.03	0.03	−0.01	0.08	0.06	0.07	0.04	0.12	0.03
$UT_{RegionMean}$	0.02	0.00	0.03	0.00	0.02	0.02	0.05	0.01	0.03	0.01
$LT_{RegionMean}$	0.00	0.00	0.00	0.00	0.01	0.00	0.01	0.00	0.00	0.00
$LS_{RegionStdDev}$	0.28	0.02	0.05	0.02	0.03	0.02	0.06	0.02	0.22	0.01
$UT_{RegionStdDev}$	0.04	0.01	0.01	0.01	0.01	0.00	0.01	0.00	0.03	0.00
$LT_{RegionStdDev}$	0.02	0.01	0.01	0.00	0.00	0.00	0.01	0.00	0.03	0.00

global mean constitutes about the same degree of error reduction as the temporal extension of the averaging period from month to year.

[61] Since CHAMP nearly samples one full diurnal cycle within one season and nearly three diurnal cycles within 1 year the LTC reduces most strongly for CHAMP: it decreases by more than a factor of two from monthly 60° sector to seasonal zonal means. The stability of simMetOp's orbit is reflected in the comparatively small decrease in LTC when increasing the averaging period. This small decrease is in this case to be attributed to the increasingly larger number of profiles which enters the SE calculation.

[62] The resolution-specific SE and LTC of seasonal means and annual means are similar for both satellites but it is evident that a larger number of profiles further reduces the LTC of a drifting satellite, whereas it "saturates" to a residual small long-term constant bias for Sun-synchronous satellites (∼0.04 K in annual mean for MetOp).

3.3. Influence of Spatial and Temporal Climatological Resolution

[63] Beyond the focus on the resolution-specific mean SE and LTC, the implications of averaging over of larger spatial regions have been studied. The 2-years average of region-averaged SE and region-averaged LTC, calculated for the same geographical regions as used for the resolution-specific estimation in section 3.2.1, are shown in Table 3. As the most salient (and expected) feature, essentially random errors are averaged out, so that region-averaged values are significantly smaller compared to resolution-specific ones.

[64] The 2-years average of the region-averaged SE is slightly positive for all satellites in all regions following from the positive SE arising at high latitudes predominantly in winter (see Figures 2 and 3) and from the systematic positive SE in the tropopause region. Since the sampling error depends on temperature variability, strongest variations occur at high latitudes. MetOp's SE in the tropical lower stratosphere is significantly larger compared to CHAMP, which is essentially zero (0.01 K is considered the limit of accuracy for quantitative interpretation, i.e., ∼0.01 K and below is "essentially zero"). It originates mainly from its LTC.

[65] The region-averaged LTC shows the difference between the Sun-synchronous satellite MetOp and the non-Sun-synchronous satellite CHAMP in the lower stratosphere. The 2-years average of the region-averaged LTC of MetOp is negative in the Southern Hemisphere but positive in the tropics (most pronounced) and the Northern Hemisphere, while the 2-years average of CHAMP's region-averaged LTC is essentially zero.

[66] Two-years averages for the whole global UTLS region yield a region-averaged SE of 0.05 K (realCHAMP), 0.04 K (simCHAMP) and 0.07 K (simMetOp), respectively. These positive SE again can be attributed to the positive SE around the tropopause and especially to the positive SE in hemispheric winter. The UTLS 2-years average LTC of both realCHAMP and simCHAMP is found zero (0.00 K), while MetOp's LTC settles down at the stable nonzero value of 0.03 K, because of the residual hemispheric asymmetry of the LTC as noted above and seen in Table 3.

4. Summary and Conclusions

[67] The study investigated the local time influence in single-satellite RO climatologies, comparing the case of Sun-synchronous (MetOp) and non-Sun-synchronous (CHAMP) satellites. The results showed that the local time of RO events has a minor but appreciable and clearly understandable influence on the sampling error of large-scale single satellite RO climatologies. The characteristics

of the local time component are dependent on the satellite's orbit.

[68] The RO events' local time from satellites in Sun-synchronous orbits keeps constant and the resulting error is influenced by the event local times. Since the magnitude of local time influences is also dependent on the number of profiles, this magnitude decreases with a larger number of measurements. Nevertheless, it leaves a small long-term constant bias in the climatology resolved into 18 latitude bands, which was estimated to be $\sim$0.04 K in annual mean for MetOp.

[69] Non-Sun-synchronous satellites are able to sample an entire diurnal cycle if the averaging period is long enough. The sampling error's local time-dependent part then becomes very small and even negligible (<0.01 K) given an adequate number of measurements.

[70] All estimated values of the local time component error represent a lower limit because the allocation of colocated ECMWF profiles to one of four UTC time layers broadens the respective local time distribution in the estimation process. However, since the diurnal cycle up to the second harmonics (semidiurnal variations) is captured by the estimation, any residual delta error is expected to be of first order (10% level) only.

[71] RO measurements can make a unique contribution to climate monitoring. For Sun-synchronous orbits, where it is imaginable that a very small drifting rate could superimpose a small pretended trend, it is thus of high importance that the orbit is maintained at nominal local time as done for the MetOp satellite series.

[72] Since the long-term bias is closely connected with the equator crossing time it is necessary to act with caution, and considering cross calibration, when comparing climatologies from Sun-synchronous satellites with different equator crossing time.

[73] Furthermore, we have as a baseline assumed that the diurnal cycle does not systematically change over time. For surface air temperature there is evidence that this is not correct in the longer-term under global warming [*Vose et al.*, 2005; *Easterling et al.*, 2006], and it is possible that transient change also occurs at UTLS height levels. While such slow global transient change will not be a problem during MetOp's life time it is necessary to be aware of this potential effect over longer periods and to have also non-Sun-synchronous RO satellites in place, which cover the diurnal cycle.

[74] All results in this study have been obtained for single satellite measurements. Since the sampling error and its local time component are highly dependent on the number of measurements they can be reduced when the number of platforms performing measurements is increased. In April 2006, the satellite mission FORMOSAT-3/COSMIC (Constellation Observing System for Meteorology, Ionosphere and Climate, [*Rocken et al.*, 2000]) was launched into a low Earth orbit; the final orbital constellation of the six satellites (altitude of 800 km and plane separation in ascending node of 30°) will be achieved by the end of 2007.

[75] The satellites, in planes with 72° inclination and different local times of equator crossing will acquire about 2500 RO events per day and thereby will strongly enhance the measurement's density over single satellites.

[76] Each single FORMOSAT-3/COSMIC satellite (in final orbit) having a drifting rate of about $-2°$/day, relative to the Earth's mean motion of about $+1°$/day, leads for the six satellites with 30° orbital plane spacing to sample one full diurnal cycle within 10 days at low and midlatitudes. Because of orbital geometry, it takes longer to sample a full diurnal cycle at high latitudes, but within one month the diurnal cycle is sampled very well everywhere. The sampling error from the FORMOSAT-3/COSMIC constellation can thus be expected to be reduced by a considerable degree for the climatological resolutions baselined in this study and the local time-dependent component will be negligible.

[77] Even for single satellite climatologies, however, the overall evidence is that monthly zonal mean climatologies of high accuracy (sampling error smaller than 0.3 K), with the local time component being a minor part (smaller than 0.1 K to 0.15 K), can be obtained. This underpins the utility of RO data for long-term monitoring of global climate variability and change.

[78] **Acknowledgments.** The authors are grateful to GeoForschungsZentrum Potsdam (in particular to J. Wickert and T. Schmidt), Germany, for providing CHAMP radio occultation data and to the European Centre for Medium-Range Weather Forecasts for access to ECMWF analysis data. Thanks are also due to M. Borsche, A. Gobiet, and A. K. Steiner for valuable scientific discussions and to J. Fritzer and J. Ramsauer (all WegCenter/University of Graz) for technical support concerning the EGOPS software. The work was supported by the Austrian Science Fund (FWF) under research grant P18837 (CLIMROCC project).

References

Boain, R. J. (2005), A-B-Cs of Sun-synchronous orbit mission design (AAS 04-108), in *Spaceflight Mechanics 2004—Part I.*, edited by S. L. Coffey et al., pp. 85–104, Univelt, Inc., San Diego, Calif.

Borsche, M., A. Gobiet, A. K. Steiner, U. Foelsche, G. Kirchengast, T. Schmidt, and J. Wickert (2006), Pre-operational retrieval of radio occultation based climatologies, in *Atmosphere and Climate: Studies by Occultation Methods*, edited by U. Foelsche, G. Kirchengast, and A. K. Steiner, pp. 315–324, Springer, Berlin.

Borsche, M., G. Kirchengast, and U. Foelsche (2007), Tropical tropopause climatology as observed with radio occultation measurements from CHAMP compared to ECMWF and NCEP analyses, *Geophys. Res. Lett.*, *34*, L03702, doi:10.1029/2006GL027918.

Easterling, D. R., B. Gleason, R. S. Vose, and R. J. Stouffer (2006), A comparison of model produced maximum and minimum temperature trends with observed trends for the 20th and 21th centuries, paper presented at 18th Conference on Climate Variability and Change, Session 5: Climate Modeling: Studies of Climate Change on 01.02.2006, Am. Meteorol. Soc., Atlanta, Ga.

Foelsche, U., A. Gobiet, A. K. Steiner, M. Borsche, J. Wickert, T. Schmidt, and G. Kirchengast (2006), Global climatologies based on radio occultation data: The CHAMPCLIM project, in *Atmosphere and Climate: Studies by Occultation Methods*, edited by U. Foelsche, G. Kirchengast, and A. K. Steiner, pp. 303–314, Springer, Berlin.

Gobiet, A., U. Foelsche, A. K. Steiner, M. Borsche, G. Kirchengast, and J. Wickert (2005), Climatological validation of stratospheric temperatures in ECMWF operational analyses with CHAMP radio occultation data, *Geophys. Res. Lett.*, *32*, L12806, doi:10.1029/2005GL022617.

Hajj, G. A., E. R. Kursinski, L. J. Romans, W. I. Bertiger, and S. S. Leroy (2002), A technical description of atmospheric sounding by GPS occultation, *J. Atmos. Sol. Terr. Phys.*, *64*, 451–469.

Hajj, G. A., C. O. Ao, P. A. Iijima, D. Kuang, E. R. Kursinski, A. J. Mannucci, T. K. Meehan, L. J. Romans, M. de la Torre Juarez, and T. P. Yunck (2004), CHAMP and SAC-C atmospheric occultation results and intercomparisons, *J. Geophys. Res.*, *109*, D06109, doi:10.1029/2003JD003909.

Hoffmann-Wellenhof, B., H. Lichtenegger, and J. Collins (1997), *GPS Theory and Practice*, 389 pp., Springer, New York.

Kirchengast, G., S. Schweitzer, J. Ramsauer, and J. Fritzer (2004), End-to-end Generic Occultation Performance Simulator Version 5 (EGOPS5) software user manual (overview, reference, and file format manual), *Tech. Rep. ESA/ESTEC 6/2004*, Inst. for Geophys., Astrophys. and Meteorol., Univ. of Graz, Graz, Austria.

Kirk-Davidoff, D., R. M. Goody, and J. G. Anderson (2005), Analysis of sampling errors for climate monitoring satellites, *J. Clim.*, *18*, 810–822, doi:10.1175/JCLI-3301.1.

Kursinski, E. R., G. A. Hajj, J. T. Schofield, R. P. Linfield, and K. R. Hardy (1997), Observing Earth's atmosphere with radio occultation measurements using the Global Positioning System, *J. Geophys. Res.*, *102*, 23,429–23,465.

Lackner, B. C., and B. Pirscher (2005), Climate diagnostics in radio occultation temperature climatologies of CHAMP and ECMWF, *Tech. Rep. Sci. Rep. 7/2005*, Wegener Cent. for Clim. and Global Change, Univ. of Graz, Graz, Austria.

Larson, W. J., and J. R. Wertz (Eds.) (1997), *Space Mission Analysis and Design, Space Technology Library*, 865 pp., Kluwer Acad., Dordrecht, Netherlands.

Leroy, S. S. (2001), The effects of orbital precession on remote climate monitoring, *J. Clim.*, *14*, 4330–4337, doi:10.1175/1520-0442(2001)014<4330:TEOOPO>2.0.CO;2.

Leroy, S. S., J. A. Dykema, and J. G. Anderson (2006), Climate benchmarking using GNSS occultation, in *Atmosphere and Climate: Studies by Occultation Methods*, edited by U. Foelsche, G. Kirchengast, and A. K. Steiner, pp. 287–302, Springer, Berlin.

Loiselet, M., N. Stricker, Y. Menard, and J.-P. Luntama (2000), GRAS—Metop's GPS-based atmospheric sounder, *ESA Bull.*, *102*, 38–44.

Mears, C. A., and F. J. Wentz (2005), The effect of drifting measurement time on satellite-derived lower tropospheric temperature, *Science*, *309*, 1548–1551.

Rocken, C., Y.-H. Kuo, W. Schreiner, D. Hunt, S. Sokolovskiy, and C. McCormick (2000), COSMIC system description, *Terr. Atmos. Oceanic Sci.*, *11*, 21–52.

Salby, M. L., and P. Callaghan (1997), Sampling error in climate properties derived from satellite measurements: Consequences of undersampled diurnal variability, *J. Clim.*, *10*, 18–36.

Steiner, A. K., G. Kirchengast, U. Foelsche, L. Kornblueh, E. Manzini, and L. Bengtsson (2001), GNSS occultation sounding for climate monitoring, *Phys. Chem. Earth*, *26*(3), 113–124.

Vose, R. S., D. R. Easterling, and B. Gleason (2005), Maximum and minimum temperature trends for the globe: An update through 2004, *Geophys. Res. Lett.*, *32*, L23822, doi:10.1029/2005GL024379.

Wickert, J., et al. (2001), Atmosphere sounding by GPS radio occultation: First results from CHAMP, *Geophys. Res. Lett.*, *28*, 3263–3266.

Wickert, J., G. Beyerle, T. Schmidt, C. Marquardt, R. König, L. Grunwaldt, and C. Reigber (2003), GPS radio occultation with CHAMP, in *First CHAMP Mission Results for Gravity, Magnetic and Atmospheric Studies*, edited by C. Reigber and P. S. H. Lühr, pp. 371–383, Springer, Berlin.

Wickert, J., T. Schmidt, G. Beyerle, R. König, C. Reigber, and N. Jakowski (2004), The radio occultation experiment aboard CHAMP: Operational data analysis and validation of vertical atmospheric profiles, *J. Meteorol. Soc. Jpn.*, *82*, 381–395.

Wickert, J., T. Schmidt, G. Beyerle, G. Michalak, R. König, S. Heise, and C. Reigber (2006), GPS radio occultation with CHAMP and GRACE: Recent results, in *Atmosphere and Climate: Studies by Occultation Methods*, edited by U. Foelsche, G. Kirchengast, and A. K. Steiner, pp. 3–16, Springer, Berlin.

U. Foelsche, G. Kirchengast, B. C. Lackner, and B. Pirscher, Wegener Center for Climate and Global Change, University of Graz, Leechgasse 25, A-8010 Graz, Austria. (barbara.pirscher@uni-graz.at)